HEDL-SA-807

CONF-760203--7

VOID-γ' PRECIPITATE INTERACTIONS IN EXPERIMENTAL NICKEL-BASE SUPERALLOYS

D. S. Gelles, M. K. Korenko and L. E. Thomas

January 1976

Paper to be presented at Conference on Alloy Behavior in Advanced Power Systems in Las Vegas, Nevada, February 22-26, 1976.

This paper is based on work performed by Hanford Engineering Development Laboratory, Richland, Washington, operated by Westinghouse Hanford Company, a subsidiary of Westinghouse Electric Corporation, under United States Energy Research and Development Administration Contract E(45-1)-2170.

VOID-γ' PRECIPITATE INTERACTIONS IN EXPERIMENTAL NICKEL-BASE SUPERALLOYS

D. S. Gelles, M. K. Korenko and L. E. Thomas

The National Alloy Development Program has been established to design or select new materials for duct and fuel cladding in breeder reactors. Void formation during neutron irradiation is a major challenge which must be overcome and controlled in order to optimize the breeding capacity of this reactor design. The work under discussion represents a small portion of the ongoing effort to understand and control the process of void swelling. In these experiments void formation was induced by irradiation with 1.0 MeV electrons in the HVEM. Since the damage rate in the HVEM is three orders of magnitude faster than that produced in the core of reactors we are able to observe void formation on an accelerated time scale. Despite the obvious differences between a single atom displacement produced by 1 MeV electrons and displacement cascades produced by neutrons, we are able to observe remarkable similarities in void distributions and swelling rates between the two irradiation environments.

Gamma-prime strengthened Fe-Ni-Cr superalloys are the prime candidates for duct and cladding applications because of their high strength and acceptable sodium compatibility. Since γ'/γ mismatch is a major variable utilized to control the coherency strengthening in these materials, the effect of γ'/γ mismatch on void swelling had to be ascertained. The alloys irradiated in the investigation were developed by Loomis, Freeman and Sponseller to study the effects of molybdenum additions on the structure and properties of γ' in nickel rich superalloys. The five alloys selected from this series scan the full available range of γ' misfit (from +.72% to -.25%) with minimal variations in chemistry.

SLIDE 1

The alloys selected are illustrated in the first slide. Molybdenum additions to the two base compositions of (1% Al, 3.5% Ti) and (4.5% Al, 0% Ti) provide a large range of misfits with some variation in γ' weight fraction. This range of misfits is brought about by a balancing of the partitioning of Ti to γ' (expanding the lattice parameter of γ') versus a partitioning of Mo to the matrix (expanding the lattice parameter of γ).

After aging for 112 hours at 927°C, the microstructure had developed as shown. For high positive and negative misfits, the γ' morphology is cubic as predicted by Hagel and Beattie. One interesting observation is that these cubes tend to align in "stringers" thus reducing the long range coherency misfit stresses in the matrix. Smaller misfits over the ranges of +0.21 to +0.03% result in spherical precipitate morphologies as expected.

Irradiation with 1 MeV electrons at 600°C produced void swelling in all five alloys. These specimens were injected with 5 appm helium prior to the irradiation to enhance void nucleation as part of our normal procedure.

SLIDE 2

The void distribution in the +.72% misfit alloy is illustrated at two dose levels in this slide. (The notation dpa denotes displacement per atom. At an irradiation rate of 15 dpa per hour these two micrographs represent structures after 20 and 60 minutes.) At the lower dose, voids form only in the matrix, well away from the γ' particles. After 15 dpa the swelling was high in the matrix and voids were developing adjacent to the γ' particles, but no voids were observed <u>within</u> γ' particles. It would be difficult to pinpoint the relative void/γ' distributions from the inspection of 2-D micrographs of 3-D structures; however, these observations were all verified by stereo analysis.

SLIDE 3

The alloy with +.21% misfit swelled at approximately the same rate as the higher misfit alloy; however, there were significant differences in the void distribution. Voids formed first in areas adjacent to but outside the γ' particles as shown at 1.25 dpa. At a dose of 15 dpa, extensive void nucleation and growth occurred in the matrix; however, once again, voids did not form within the γ' particles.

SLIDE 4

For a misfit of +0.09%, the voids were found to nucleate first in the vicinity of the γ' particles. Stereo microscopy demonstrated that the voids were, in fact, at the interface. At higher doses, voids began to nucleate in the matrix but again voids were not observed to form in the center of the γ' particles. Note that these micrographs illustrate the swelling behavior at twice the doses shown in the previous slides. The swelling resistance of this alloy is probably related to the compositional differences between alloys rather than to any misfit effect. More specifically it appears (by comparing the relative magnitude of swelling among these five alloys) that substituting 3.5 w/o Al for Ti decreases the swelling response. (On an atomic percent basis twice as many aluminum atoms were added.)

SLIDE 5

As the misfit is decreased further to +0.03%, voids first develop within the γ' particles near the γ'/γ interface. After 30 dpa voids were also observed in the matrix. Thus, as the misfit approaches zero, the void distribution becomes more homogeneous.

SLIDE 6

The final micrograph represents the structure of the negative misfit alloy at -0.25%. For this alloy the void development has changed again. In contrast to the high positive misfit alloys, voids grow first within the γ' precipitates and it is not until higher doses that void nucleation occurs in the matrix. Thus, there is a continuous transition in void distribution as a function of γ'/γ misfit.

SLIDE 7

This slide schematically summarizes the above observations. The void structure across the interface as a function of dose is shown for each alloy condition. The swelling in the two highest positive misfit alloys is significantly greater than in the three other cases. This effect is more indicative of alloy chemistry differences than in γ'/γ misfit.

The most striking correlation, however, is the continuous change in swelling response as a function of misfit. In the high positive misfit alloys, swelling occurs only in the matrix whereas in highly negative misfit alloys, voids are generated first in the γ' and later in the matrix.

Another point illustrated in this figure is that voids in the matrix develop at higher and higher doses as the misfit becomes more negative, indicating an enhancement of the swelling incubation time either by negative misfit or by increasing molybdenum content.

SLIDE 8

This slide illustrates the variation of matrix and γ' composition for the alloys under investigation as measured by Loomis, Freeman and Sponseller.

The possibility remains that the effects which have been attributed to γ'/γ misfit may in fact be the result of differences in alloy chemistry. The swelling behavior was examined from several different approaches to establish correlations between alloy chemistry variations and the relative swelling of γ and γ'. Increasing the aluminum content of the matrix increases the matrix swelling; however, increasing the aluminum content of the γ' decreases the swelling within the precipitates. From the standpoint of the partitioning of aluminum between γ and γ', there are significant changes in void distribution while the Al partitioning coefficient is remaining relatively constant. The effect of molybdenum is assessed as follows: The matrix molybdenum content is the same in the +0.21% and the -0.25% alloy; however, there is a dramatic difference in their swelling behavior. Likewise, the +0.21% and the +0.03% alloys have comparable molybdenum contents in the γ' phase, yet they swell at different rates. Considerations of the partitioning of molybdenum also do not reveal any consistent correlations. Thus, although there will always be some uncertainty because of the differences in alloy chemistry, a detailed examination does not support a correlation based on alloy chemistry.

SLIDE 9

One way in which this chemistry effect could cloud the misfit analysis is illustrated in this slide. If the γ' and γ swell at the same rate but have different incubation times, low dose observations in which γ' is observed to swell before γ may be due to differences in the incubation time between γ and γ' (induced by composition differences which were necessary to change the γ'/γ misfit).

Misfit, however, may vary the relative incubation time of the γ'/γ through mechanisms other than alloy chemistry which will be discussed shortly.

For now, however, we must assume that chemical effects are responsible for the differences in the relative magnitude of the swelling but do not control the void distribution.

SLIDE 10

Withthat premise in mind, let us examine the various effects related to misfit which could influence the void distribution:

There is both theoretical (Bullough's theories) and experimental (swelling suppression in 316 stainless steel by cold working) evidence that dislocation densities and distribution effect swelling. These effects could be coming into play in these experiments since a variation of misfit produces differences in dislocation loop formation and eventual dislocation distribution. The next two slides illustrate some of the differences in loop distribution observed during the irradiation as γ'/γ misfit is varied.

At +.21% lattice misfit the alloy exhibited unusually rapid loop formation at the particle interfaces. At higher doses loops formed within the γ' particles as well as the matrix, but the dislocation densities of the particles appeared higher than that of the matrix.

At +0.03% misfit the loops appeared simultaneously in the matrix and at the particle surfaces.

SLIDE 11

At -.25% misfit, a few interfacial dislocations formed; however, large Frank loops were generated in the γ' particles after 30 dpa as illustrated on this slide. These differences in dislocation distribution with γ'/γ misfit could influence the void distribution.

SLIDE 12

Residual gases such as oxygen, nitrogen and hydrogen are necessary in many cases for void nucleation. The stress state resulting from the γ'/γ mismatch would be expected to give rise to a non-homogeneous distribution of these gases, thereby causing nonuniform void distributions.

Finally, the size misfit leads to a hydrostatic and shear stress state as described by Eshelby and illustrated schematically on the next slide. Shown on this slide are the expected superimposible hydrostatic stress states resulting from the size (dilatational) and coherency misfits. For a negative misfit $a_0 (\gamma') < a_0 (\gamma)$ the effect is to place the γ' under a positive hydrostatic stress (and vice versa for positive misfits). Since it is currently believed that positive stress enhances swelling and negative stress suppresses it, this stress state is consistent with the observed void distributions shown earlier. At this time, theoretical and experimental work is in progress to establish which of these mechanisms is controlling void distribution in these alloys.

Investigations of the detailed role of γ'/γ misfit has an impact on the design of new materials for reactor applications. Maximizing γ'/γ mismatch for ex-reactor strength may not be the appropriate course of action for these alloys. If high misfit enhances swelling in a manner that reduces the misfit stresses then the bulk of the ex-reactor strength will be lost in an irradiation environment. One additional important question that needs attention is "How detrimental is a void layer at the γ'/γ interface to mechanical properties?" Work is ongoing in the Alloy Development Program to answer this and other questions crucial to alloy design.

VOID- γ' PRECIPITATE INTERACTIONS

MICROSTRUCTURES BEFORE HVEM IRRADIATION

COMPOSITION:	Ni-14Cr-1Al-3.5Ti	Ni-14Cr-1Al-3.5Ti-8Mo	Ni-14Cr-4.5Al	Ni-14Cr-4.5Al-2Mo	Ni-14Cr-4.5Al-8Mo
MICROSTRUCTURE:	A	B	C	D	E
WEIGHT FRACTION γ':	5%	8%	5%	8%	17%
MISFIT*:	+0.72%	+0.21%	+0.09%	+0.03%	-0.25%

$$* \text{ MISFIT} = \frac{a_{\gamma'} - a_{\gamma}}{a_{\gamma}}$$

2

VOID SWELLING : + 0.72 % MISFIT

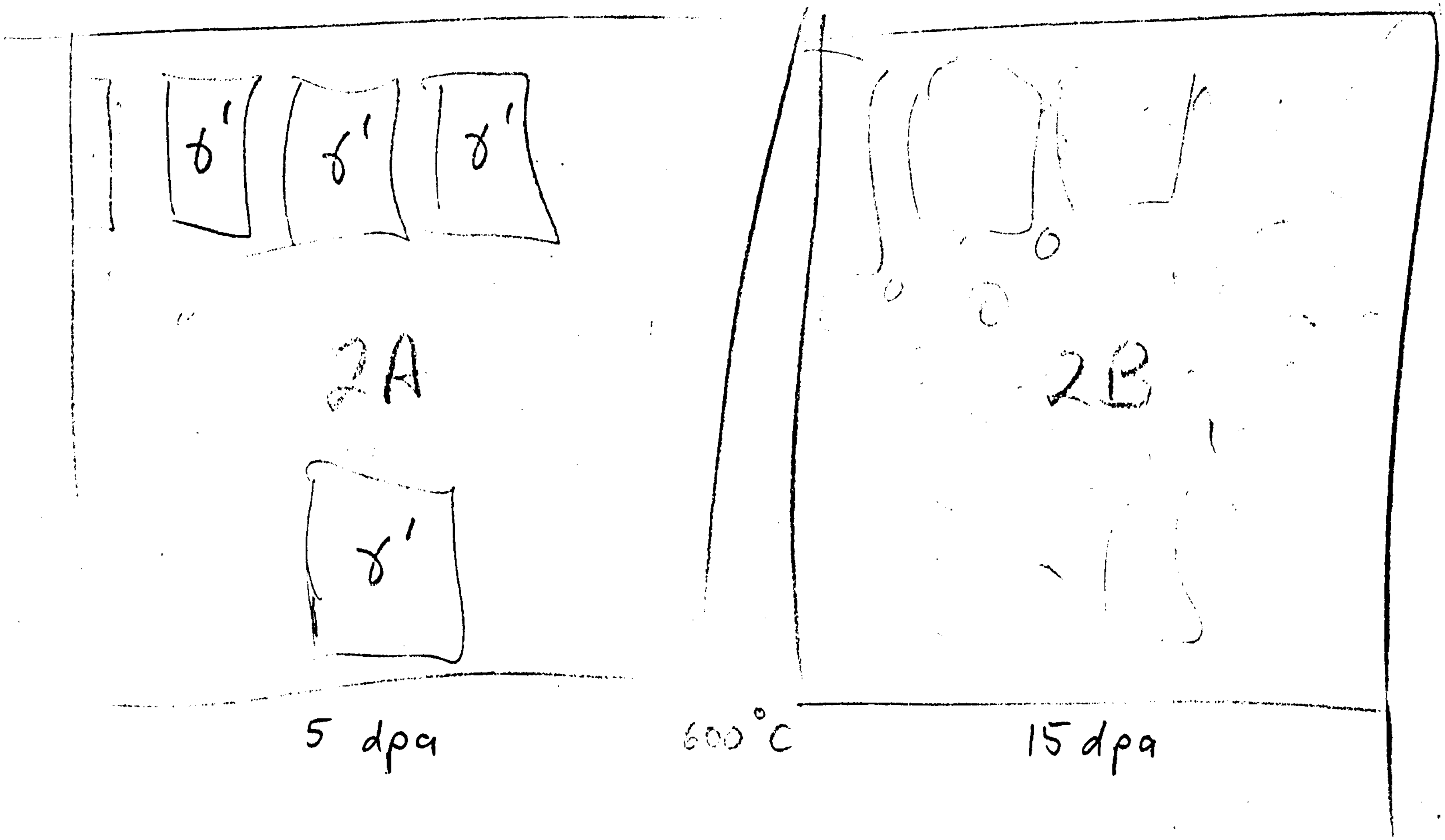

VOID SWELLING : +0.21% MISFIT

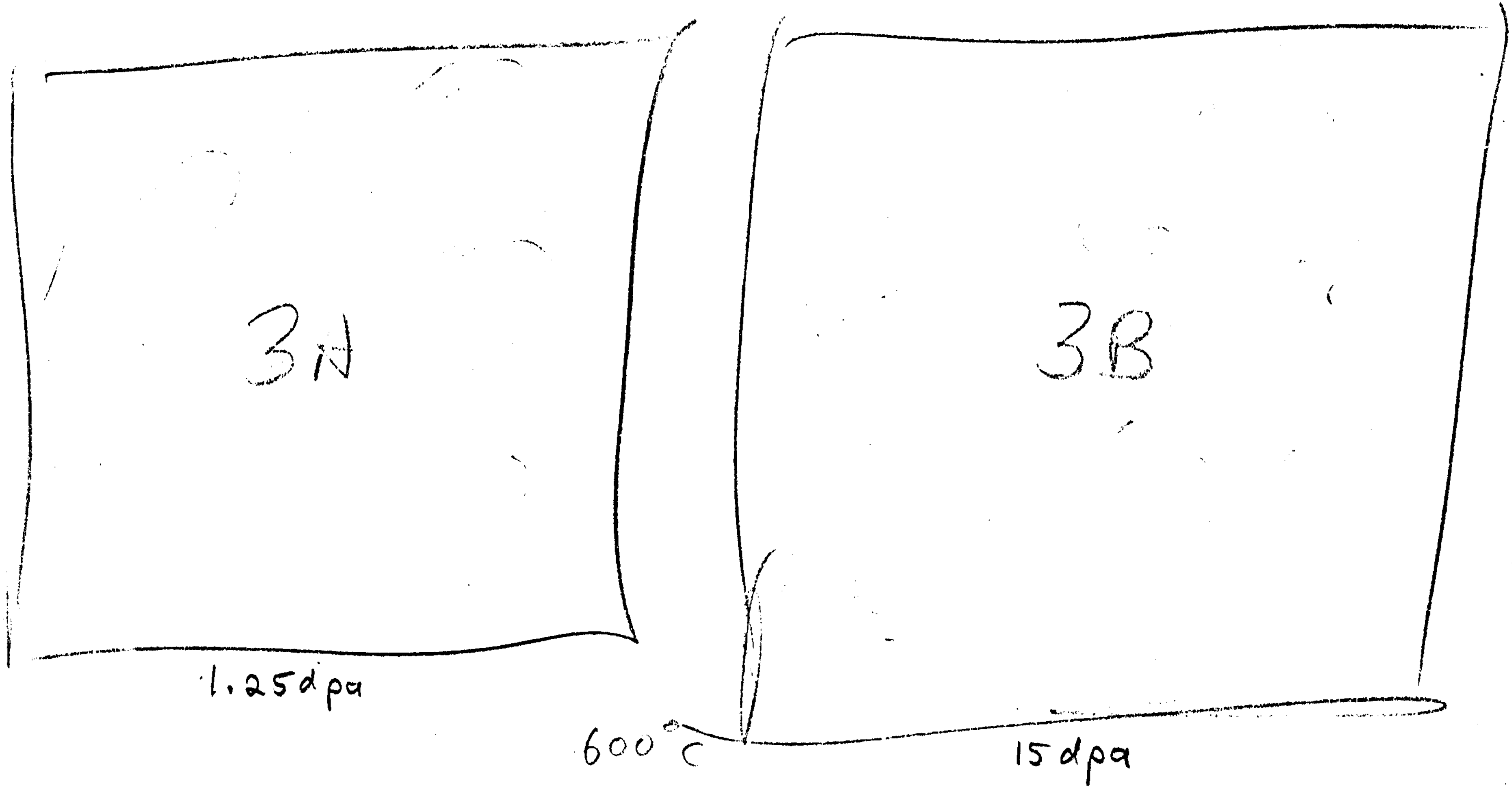

VOID SWELLING : + 0.09 % MISFIT

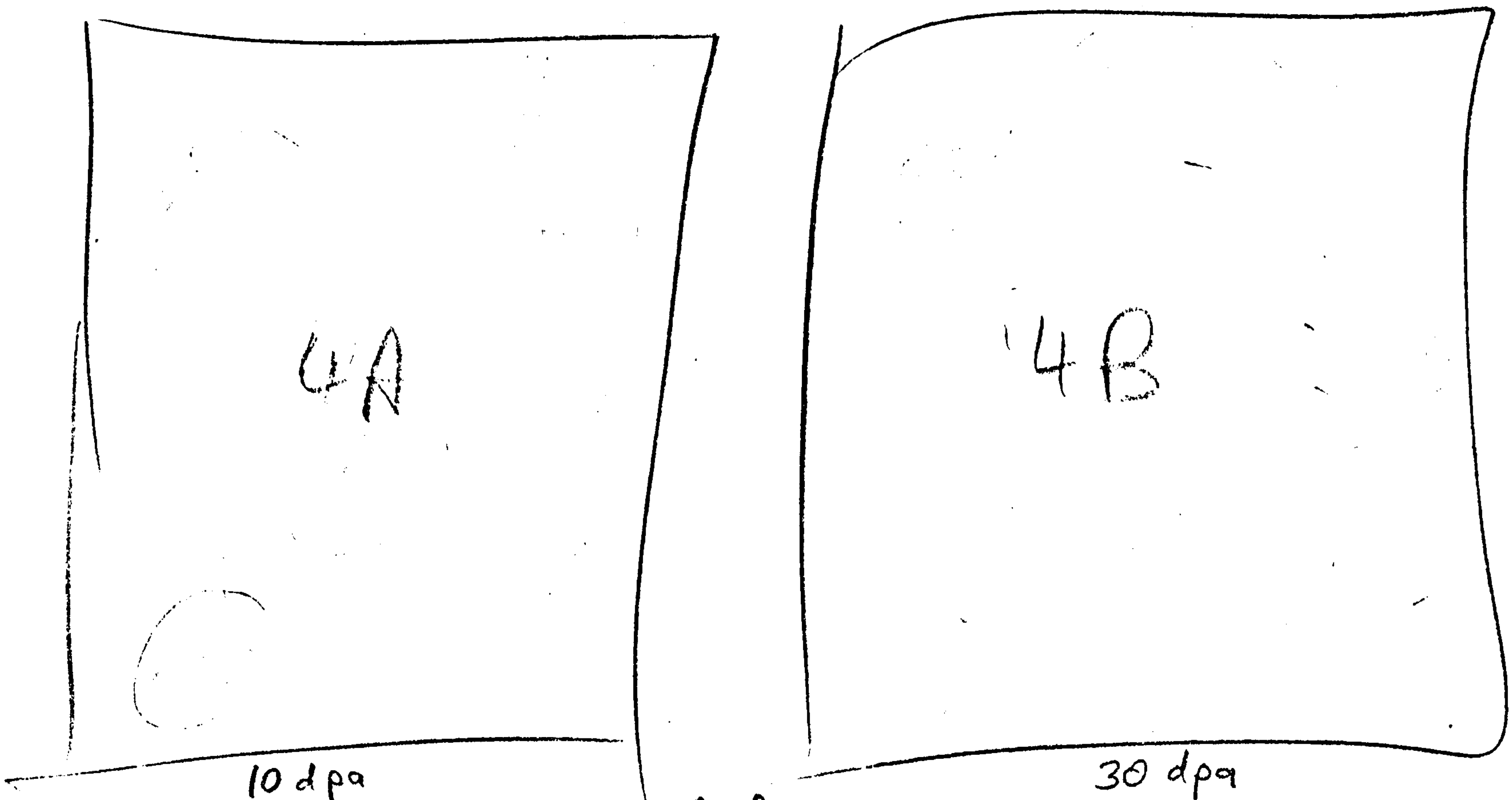

10 dpa

30 dpa

600°C

VOID SWELLING +0.03 % MISFIT

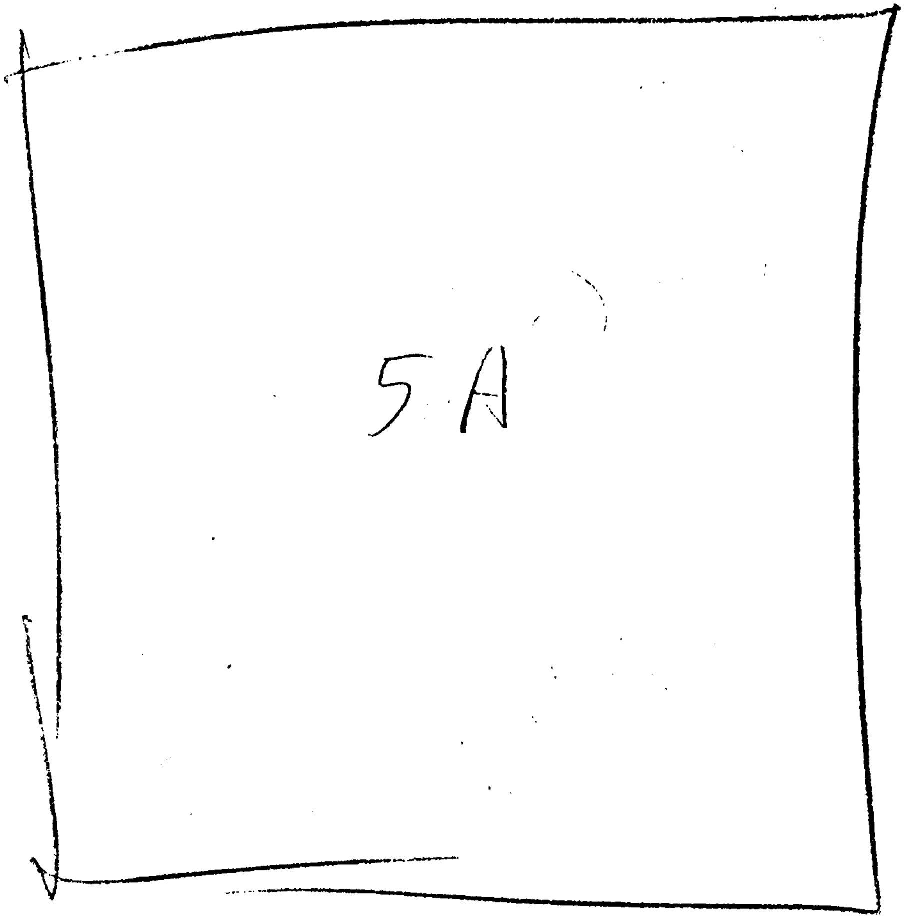

5 dpa

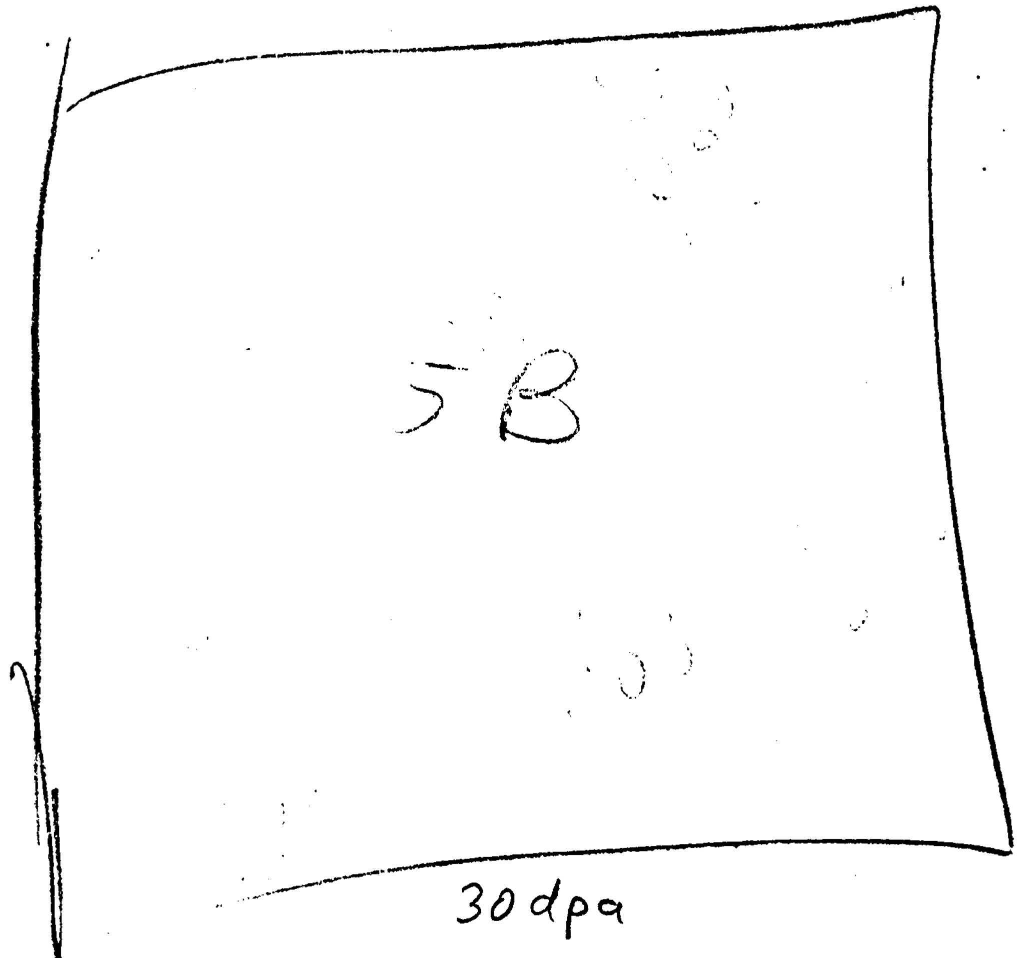

30 dpa

600°C

VOID SWELLING : – 0.25% MISFIT

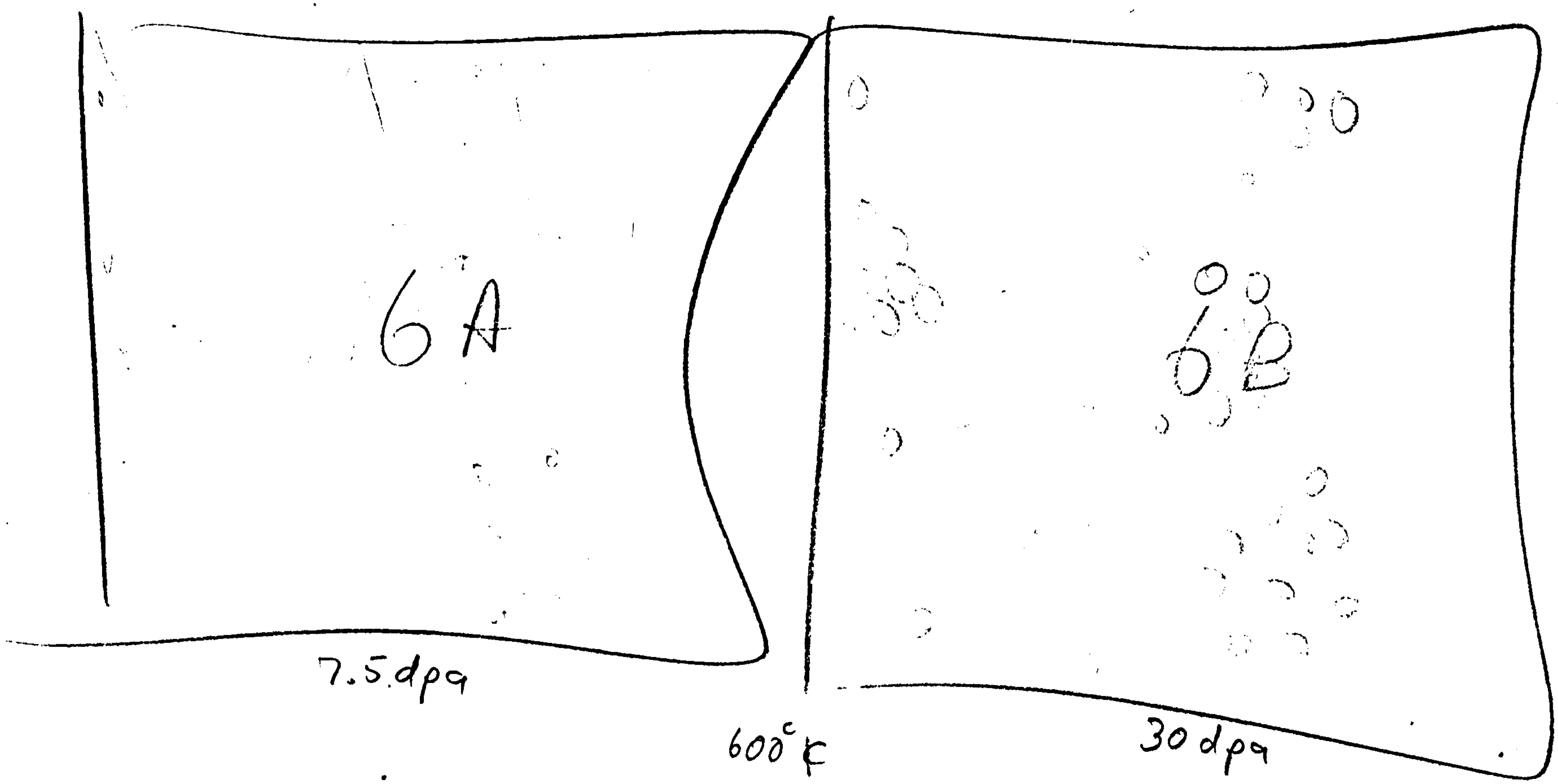

SWELLING OBSERVATIONS SUMMARIZED

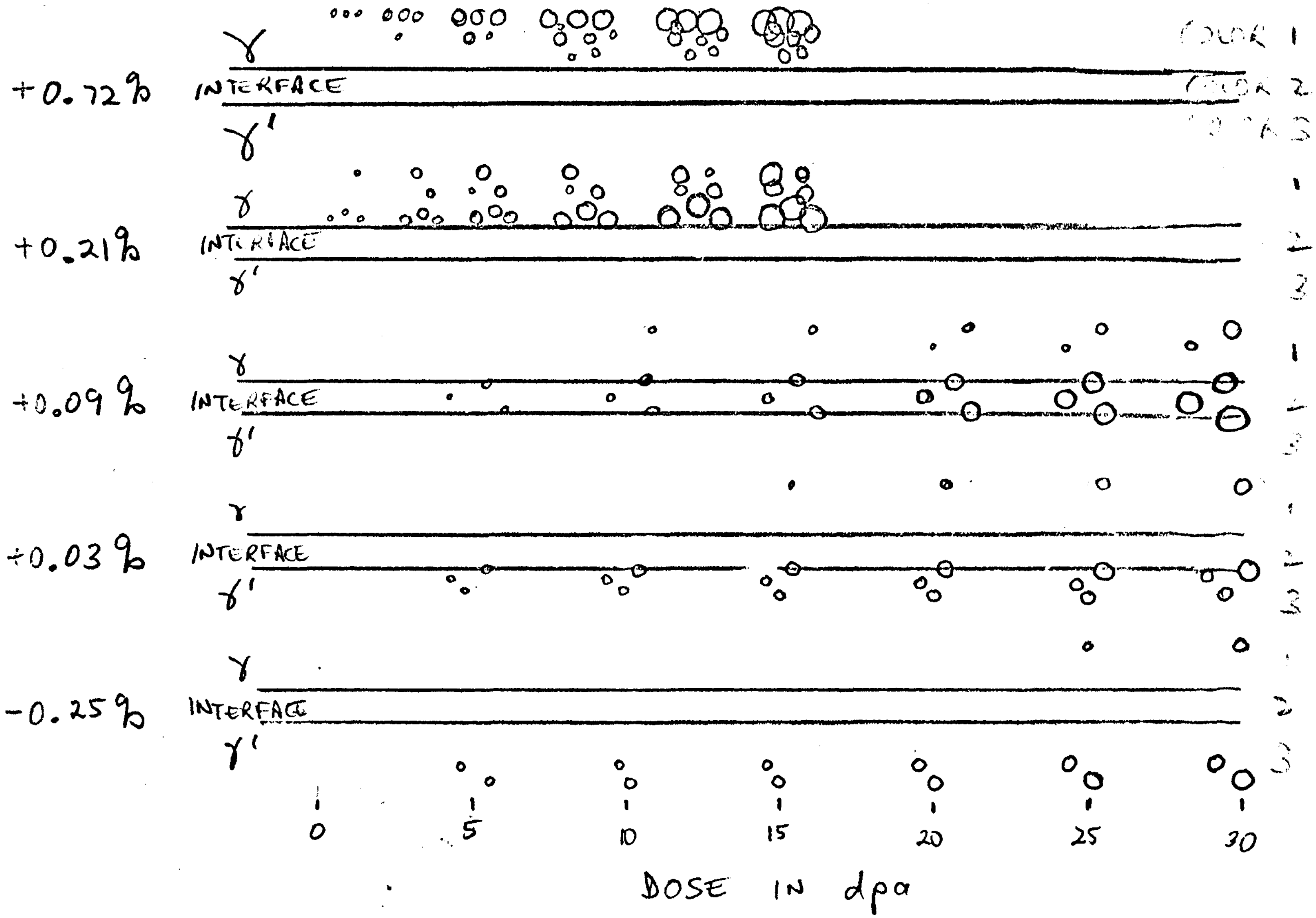

MICROSTRUCTURE CHEMISTRY

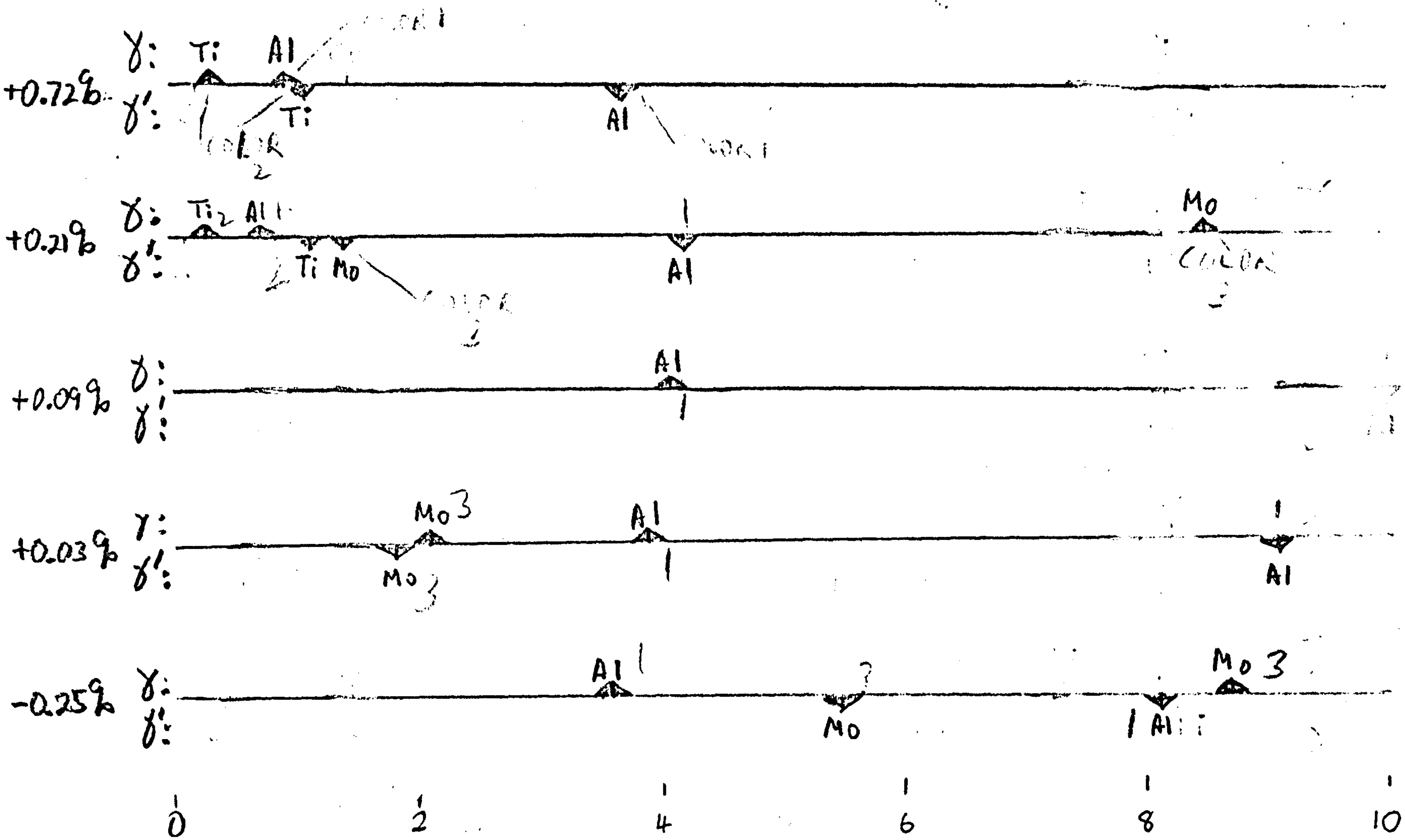

WEIGHT PERCENT

CHEMICAL EFFECT ON INCUBATION DOSE FOR SWELLING

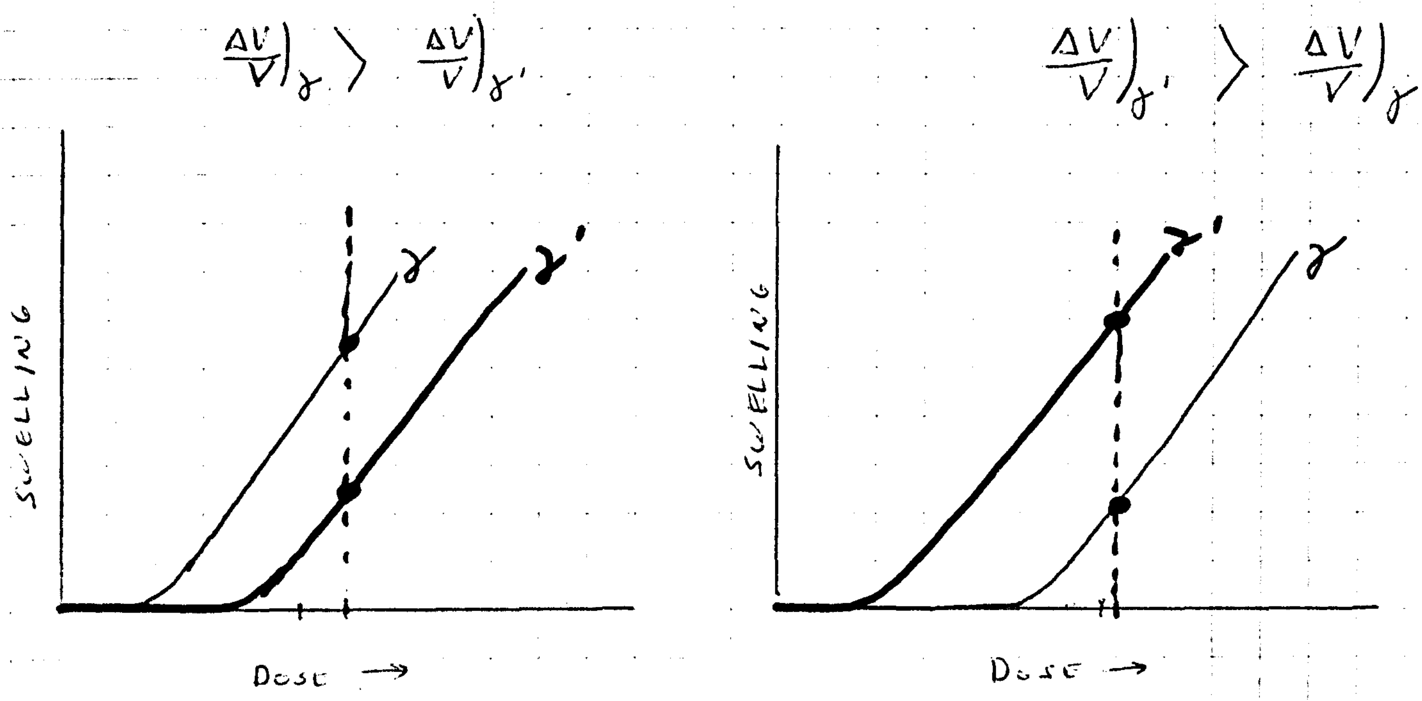

(A)

(B)

(10)

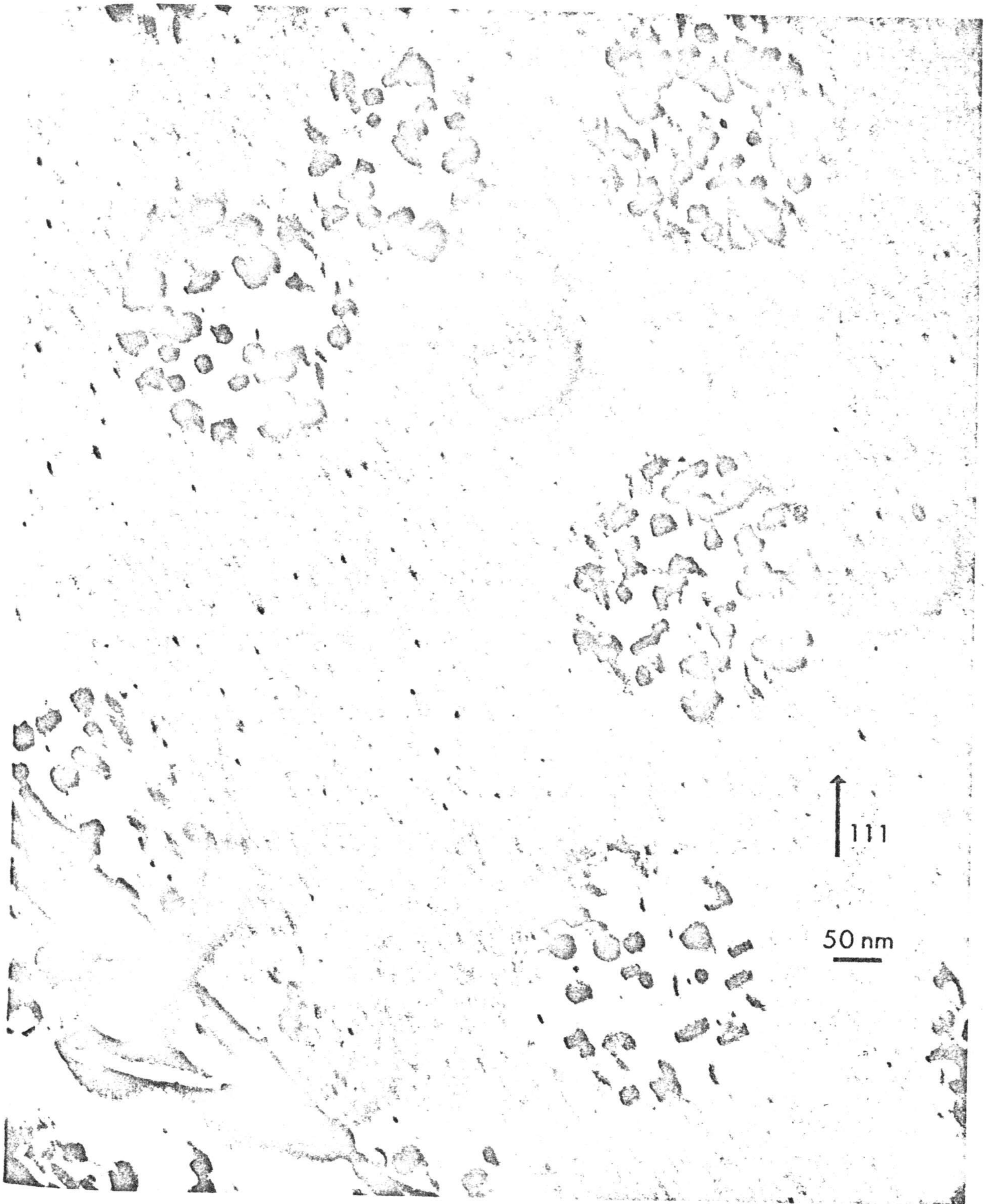

FIGURE 224a. Dislocation structure at 600°C after low dose in a γ' Series 2 Alloy #16 HVEM irradiation. Dislocation loops have formed first at γ' particle interfaces.

11

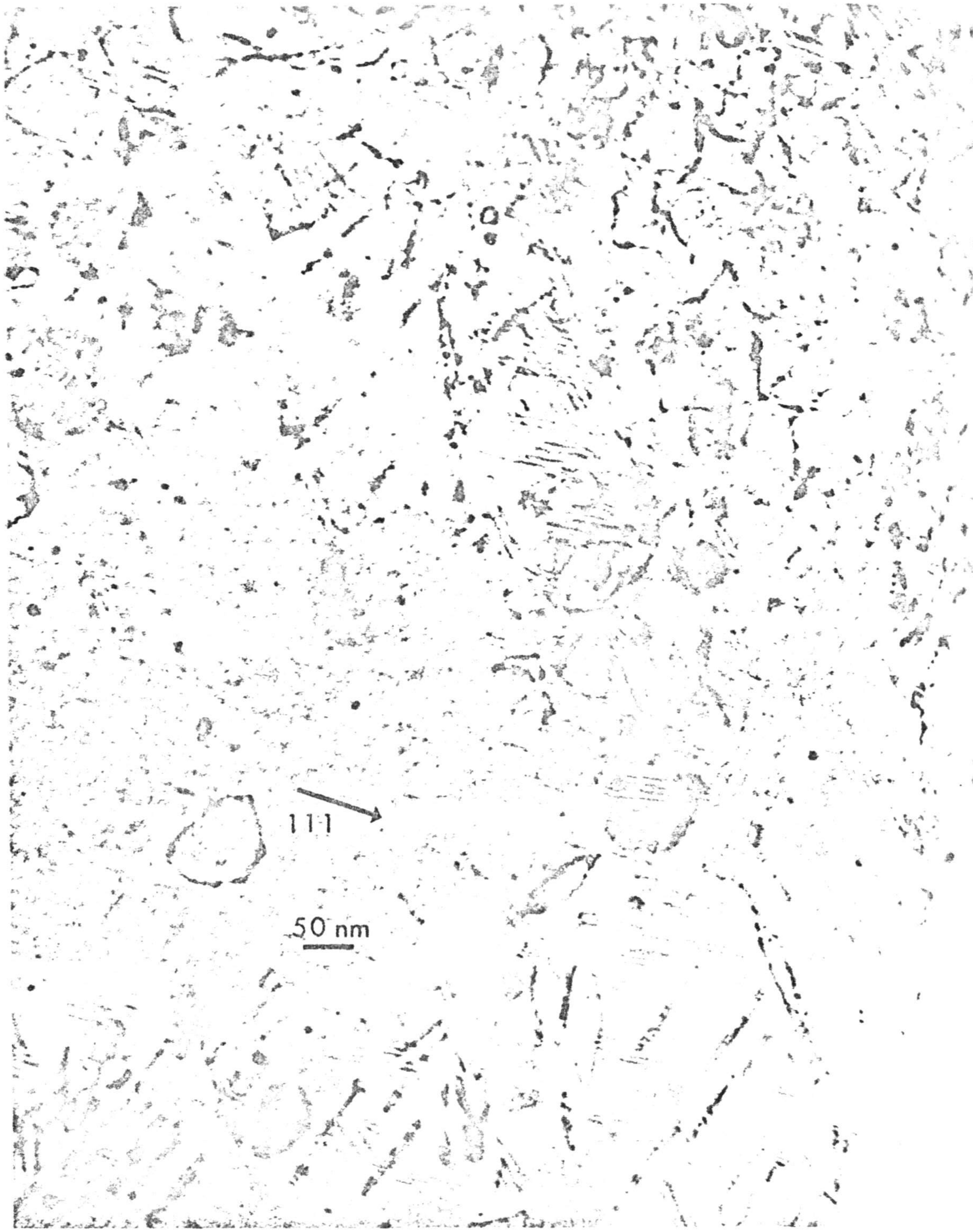

FIGURE 223a. Dislocation loop structure at 600°C produced at the edge of the irradiated region after a 30 dpa HVEM irradiation in Series 2 Alloy #8. The dislocation structure is predomin within γ' particles.

MISFIT STRESSES